Differentiating fundamental structural units during the dissolution of zeolite A†

L. Itzel Meza,* Michael W. Anderson* and Jonathan R. Agger

Received (in Cambridge, UK) 29th January 2007, Accepted 5th March 2007
First published as an Advance Article on the web 21st March 2007
DOI: 10.1039/b701301a

***In situ* atomic force microscopy (AFM) is used to differentiate temporally both structure and mechanism in the removal of fundamental structural units during the dissolution of zeolite A.**

Thermodynamics of growth and dissolution processes of crystals are directly influenced by the conditions to which the crystals are exposed. The rates at which these phenomena occur during growth determine the final facets observed on the crystals. Zeolite crystallisation processes are usually studied by a combination of X-ray diffraction and optical microscopy to determine bulk growth rates. Other techniques such as light scattering and electron microscopy have been used to determine individual crystal sizes. Growth rates from 0.01 and up to 2.20 μm h^{-1} have been reported for zeolite A. The specific rates depend upon the experimental growth conditions.[1–4] Dissolution processes on zeolite A crystals have only been studied on bulk samples rather than individual crystals.[5,6] A combination of *in situ* and *ex situ* AFM allows real-time surface processes to be monitored and to date, studies of materials such as quartz,[7,8] calcite,[9–13] gibbsite,[14] and heulandite[15] have been reported. In this first *in situ* AFM study of zeolite A the crystal surface was monitored, in real time, during exposure to alkaline solutions of differing concentrations, undersaturated mother-liquor and acetic and sulfuric acids.‡ The important features of dissolution under the first two regimes are given respectively (Fig. 1 and 2). The dissolution process is revealed to occur in at least two steps and the results give important clues about the relative stability of different structural units.

First we consider zeolite A dissolution in 0.5 M NaOH (Fig. 1). AFM micrographs were recorded, *in situ* under static solution, every 3 min in order to observe the temporal surface reconstruction. In this communication we present key event times to illustrate important aspects. A full report, showing all figures and dissolution processes, is contained elsewhere.[16] At time zero, (Fig. 1(a), measured in air) the square terraces are all 1.2 ± 0.1 nm high – equivalent to half the unit cell dimension (see Experimental section for error determination). Dissolution proceeds principally *via* terrace retreat until 31 min (Fig. 1(b)). Then, preferential opening of small holes in the initial terrace suggests the straight edge steps are more stable than the curved steps circumscribing the holes. This is in accord with the previous observation that the reverse process, *i.e.* growth of zeolite A, occurs preferentially at kink sites rather than terrace edge sites.[17] The retreating terrace, however, is only 0.9 ± 0.1 nm (*i.e.* not the full height of the original terrace). Furthermore it is evident, in particular in both Fig. 1(b) and (c), that part of the terrace remains undissolved. The height of this terrace is the remaining 0.3 ± 0.1 nm. The top terrace continues to dissolve both by terrace retreat and ultimately break up into small squares which finally disappear after 47 min (Fig. 1(f)). This phenomenon of terrace break-up is more pronounced in the sample treated with undersaturated mother-liquor (see below). The second terrace also dissolves by 0.9 ± 0.1 nm terrace retreat and eventual break-up but the retreat is halted when the terrace edge reaches the remaining 0.3 ± 0.1 nm edge from the top terrace. This 0.3 ± 0.1 nm edge is essentially unmoved from its initial position illustrating that the 0.3 nm high terrace is more stable to dissolution than the 0.9 nm high terrace. When the 0.9 nm high terrace is finally removed it is observed that another 0.9 nm high layer begins to be removed, again by terrace retreat. Consequently, AFM does not reveal the disappearance of the 0.3 nm intervening layer suggesting that this layer (which is close to the resolution of the microscope) is not removed by terrace retreat but rather by dissolution orthogonal to the surface. In summary, zeolite A dissolves under these conditions by terrace retreat of a 0.9 nm layer followed by uniform dissolution of a 0.3 nm layer.

It is important then to know the structural nature of the 0.9 and 0.3 nm layers. The only published electron microscopy work on the surface structure of zeolite A comprises electron micrographs of relatively thick crystals suggesting (100) surface termination by half β-cages. This is somewhat suspect because, as noted by the authors, the substantial crystal thickness will result in significant distortions of the micrographs.[18] The only other guidance is the theoretical work of Slater *et al.* suggesting, on energetic grounds, preferred surface units are either complete β-cages or complete double four rings (D4Rs).[19] Our work is more consistent with this explanation as the 0.3 nm layer would correspond to the removal of the top of the D4R, *i.e.* a single four ring (S4R), to leave a β-cage cage and the 0.9 nm layer would correspond to removal of a β-cage cage, less its base, to leave a D4R. In both instances this leaves an intuitively satisfying, complete cage structure intact at the surface (see Fig. 3). The nature of such structural units also accounts for the different mechanism by which each unit is dissolved. The S4R units are not linked to one another and thus it is expected that they will dissolve in an uncorrelated fashion. The β-cages are linked parallel to the surface. Consequently, the dissolution of a β-cage is linked to the dissolution of its neighbour. This coordinated dissolution results in terrace retreat.

Centre for Nanoporous Materials, School of Chemistry, The University of Manchester, Chemistry Building, Oxford Road, Manchester, UK M13 9PL. E-mail: M.Anderson@manchester.ac.uk; L.Meza@manchester.ac.uk; Fax: +44 161 275 4598; Tel: +44 161 306 4527

† Electronic supplementary information (ESI) available: Characterisation and experimental details. See DOI: 10.1039/b701301a

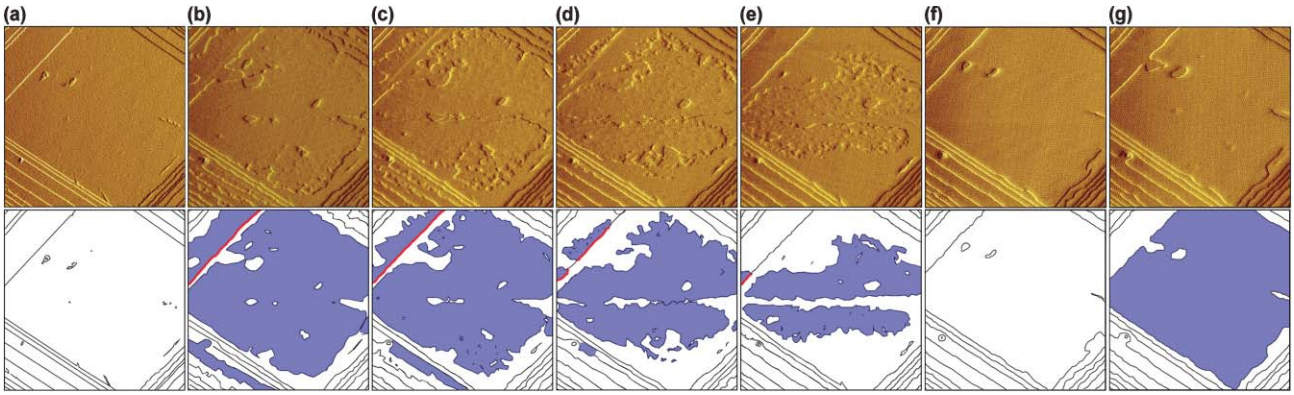

Fig. 1 4.3 × 4.3 μm^2 deflection AFM images and corresponding schematics of a zeolite A crystal dissolving under 0.5 M NaOH after (a) 0, (b) 31, (c) 33, (d) 36, (e) 38, (f) 47 and (g) 55 min. In the schematics the black and red lines correspond to step heights of 1.2 and 0.3 nm respectively, the blue areas represent layers with step heights of *ca.* 0.9 nm.

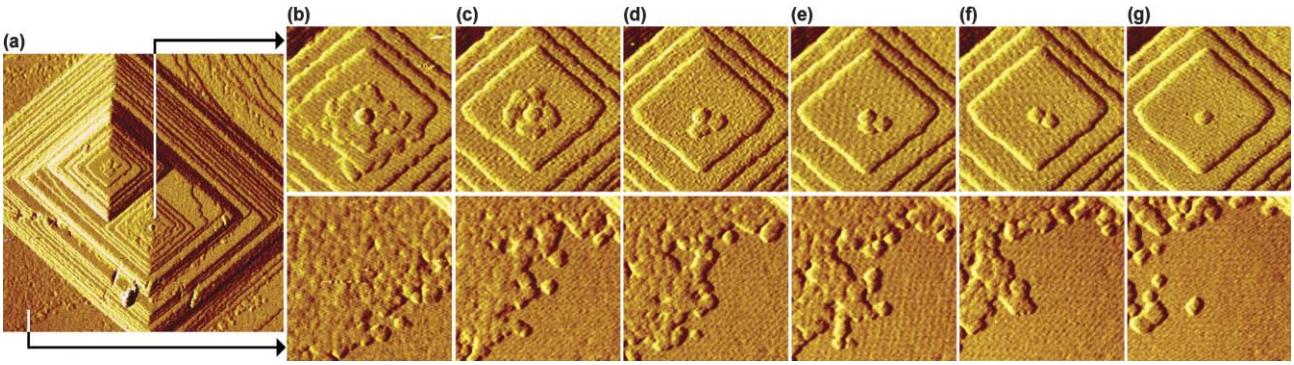

Fig. 2 Deflection AFM images of two regions of the (100) face of zeolite A dissolving under 67% diluted aqueous mother-liquor after (a) 10, (b) 15, (c) 35, (d) 55, (e) 75, (f) 95 and (g) 115 min. Micrographs with scan sizes of (a) = 5 × 5 μm^2 and (b–g) = 1 × 1 μm^2.

The final question is whether the original external surface is the D4R or the β-cage. As we are unable to observe the homogeneous removal of the 4-ring either explanation is consistent with the data and this remains an open question. The successive dissolution of layers starting either with a D4R surface or a complete β-cage surface is shown in Fig. 3. The figure also illustrates how this mechanism accounts for the periodic formation of the same lateral surface topology as the crystal is dissolved – a feature which is observed by AFM, compare Fig. 1(a) and (f). Theoretical calculations supporting the present model will be published elsewhere.[16]

A similar dissolution process is observed when zeolite A is exposed to an undersaturated mother-liquor, produced by diluting the mother-liquor to 67% of its original concentration (see Fig. 2). However, even more pronounced in this dissolution is the final break-up of the 0.9 nm high retreating terraces into small squares. The size of these squares is quite uniform, *ca.* 90 × 90 × 0.9 nm (or *ca.* 36 × 36 unit cells laterally). These squares persist before final dissolution orthogonal to the surface. This unusual feature in the dissolution of the (100) surface of zeolite A suggests that there is a decrease in the surface free energy for these 0.9 nm terraces as the lateral size decreases, until a minimum at the critical size of *ca.* 90 × 90 nm. In order to explain such phenomena it would be important to calculate expected surface free energies and also energies of attachment for such structures.

The dissolution process on the {100} face of zeolite A, observed under the different experimental conditions, was quantified by measuring the areas of terraces dissolved by the different solutions. In order to calculate dissolution rates from the different retreating terraces measured, numerical values of the slopes d[area]/dt were initially calculated from the linear stages. This number was defined as the two-dimensional (2D) rate of terrace dissolution, r, which was then used to obtain the final rate of dissolution, R, using the following expression: $R = hr/\lambda$, where R is the rate of crystal dissolution in μm s^{-1}, h is the step height of the layer that is dissolving in μm, r is the rate of 2D terrace dissolution in μm^2 s^{-1} and λ is the area spacing between the steps in μm^2. The dissolution rate, R, is conditioned by the temperature at which the experiment was conducted (formula adapted from work published by Gratz *et al.*[7])

Different rates of dissolution were obtained from the experiments conducted as part of this present work. The highest dissolution rate, 3.4 × 10^{-6} μm s^{-1}, was obtained when zeolite A crystals were exposed to a solution of 0.5 M NaOH and the lowest, 2.1 × 10^{-7} μm s^{-1}, was for exposure to a solution of mother-liquor diluted to 10% with distilled water. There is a trend observed among the experiments conducted using mother-liquor. It seems the more diluted the mother-liquor the smaller the dissolution rate obtained. This is as expected for a dilute solution where all concentrations are modified and consequently the pH is

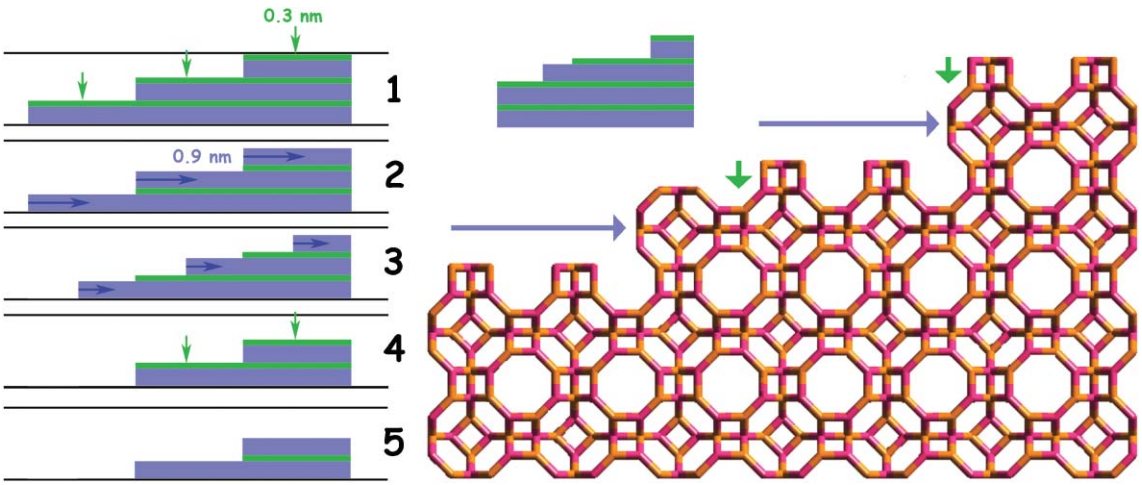

Fig. 3 Schematic illustration of the dissolution process for zeolite A under alkaline conditions. Uncorrelated removal of an S4R (green arrow) capping the D4R layer on the surface of the structure (green layer) amounts to 0.32 nm. Correlated removal of a β-cage, except the 4-ring base, (blue arrow) amounts to 0.92 nm. Layers are successively removed, 4-rings orthogonal to the surface and β-cage cages parallel to surface *via* terrace retreat. The process is either 1–2–3–4 repeat or 2–3–4–5 repeat depending on the initial exterior surface of the crystal. Note how the top surfaces of 1 and 4 or 2 and 5 are only displaced orthogonally to the surface by 1.2 nm and therefore indistinguishable by AFM, compare Fig. 1(a) and Fig. 1(f).

adjusted towards neutral. There is very little data in the literature regarding bulk dissolution with which to compare our result. However, if we make a rough comparison with the work of Čižmek *et al.*[20] who measured bulk dissolution rates in 1 M NaOH at 338 K they established linear dissolution rates approximately 200 times greater than our rates under 0.5 M NaOH at 298 K. Such a difference seems reasonable considering the milder conditions in our work.

Finally zeolite A crystals were exposed to acetic and sulfuric acid at different concentrations with pH values ranging from 2.8 to 5.0. The acid attacks not only the top layer of the surface, but also some of the layers below and as a result deep dissolution pits are formed within 2 min. The formation of dissolution pits is the result of H^+ attacking the bonds of the surface species such as Si–OH. These protons also affect the Si–O–Si and Si–O–Al species in the top aluminosilicate layers and as a consequence hydrolysis reactions take place. The effect of acidic attack is enhanced by the porosity of the zeolite, which allows H^+ to penetrate the structure and reach the internal Si–O and Al–O bonds.[16]

In summary, this study provides *in situ*, real-time evidence of the dissolution mechanism of zeolite A. It will be interesting to establish whether the mechanisms observed here for dissolution are mimicked in reverse for crystal growth, however, this question remains, as yet, unanswered. The implications of the findings in this study will affect the way we think about growth and dissolution in a wide variety of framework materials where different, but discrete, structural units grow or attach at different rates and by different mechanisms. The work underlines the importance of differentiating the fundamental processes rather than relying solely on bulk processes.

Notes and references

‡ Zeolite A crystals were synthesized from a gel with molar composition 1 SiO_2 : 2.23 Na_2O : 5.18 TEA : 0.89 Al_2O_3 : 246 H_2O which was kept at 90 °C for 10 days. Atomic force micrographs were recorded on a Nanoscope IIIa using contact mode with 0.58 N m^{-1} force constant silicon nitride tips at scan rates of 3 Hz. A syringe pump was used for the experiments conducted under continuous flow through the fluid cell. All the experiments were carried out at room temperature of about 25 °C. Errors in terrace heights were determined by measuring at least 50 separate heights.

1 S. P. Zhdanov, in *Molecular Zeolites I*, ed. E. M. Flanigen and L. B. Sand, American Chemical Society, Washington, DC, 1971, vol. 101, pp. 20–28.
2 W. Meise and F. E. Schwochow, in *Molecular Sieves*, ed. W. M. Meier and J. B. Uytterhoeven, American Chemical Society, Washington, DC, 1973, vol. 121, pp. 169–178.
3 G. J. Myatt, P. M. Budd, C. Price, F. Hollway and S. W. Carr, *Zeolites*, 1994, **14**, 190–197.
4 L. Gora, K. Streletzky, R. W. Thompson and G. D. J. Phillies, *Zeolites*, 1997, **18**, 119–131.
5 A. Čižmek, L. Komunjer, B. Subotić, M. Široki and S. Rončević, *Zeolites*, 1991, **11**, 258–264.
6 C. Kosanović, B. Subotić, V. Kaučič and M. Škreblin, *Phys. Chem. Chem. Phys.*, 2000, **2**, 3447–3451.
7 A. J. Gratz, S. Manne and P. K. Hansma, *Science*, 1991, **251**, 1343–1346.
8 M. L. Schlegel, K. L. Nagy, P. Fenter and N. C. Sturchio, *Geochim. Cosmochim. Acta*, 2002, **66**, 3037–3054.
9 P. E. Hillner, S. Manne, A. J. Gratz and P. K. Hansma, *Ultramicroscopy*, 1992, **42–44**, 1387–1393.
10 P. E. Hillner, S. Manne, P. K. Hansma and A. J. Gratz, *Faraday Discuss.*, 1993, **95**, 191–197.
11 S. Kipp, R. Lacmann and M. A. Schneeweiss, *J. Cryst. Growth*, 1994, **141**, 291–298.
12 L. E. Wasylenki, P. M. Dove, D. S. Wilson and J. J. De Yoreo, *Geochim. Cosmochim. Acta*, 2005, **69**, 3017–3027.
13 P. S. Dobson, L. A. Bindley, J. V. Macpherson and P. R. Unwin, *Langmuir*, 2005, **21**, 1255–1260.
14 C. D. Peskleway, G. S. Henderson and F. J. Wicks, *Am. Mineral.*, 2003, **88**, 18–26.
15 S. Yamamoto, S. Sugiyama, O. Matsuoka, K. Kohmura, T. Honda, Y. Banno and H. Nozoye, *J. Phys. Chem.*, 1996, **100**, 18474–18482.
16 L. I. Meza, B. Slater, M. W. Anderson and J. R. Agger, unpublished work.
17 J. R. Agger, N. Hanif and M. W. Anderson, *Angew. Chem., Int. Ed.*, 2001, **40**, 4065–4067.
18 T. Wakihara, Y. Sasaki, H. Kato, Y. Ikuhara and T. Okubo, *Phys. Chem. Chem. Phys.*, 2005, **7**, 3416–3418.
19 B. Slater, J. O. Titiloye, F. M. Higgins and S. C. Parker, *Curr. Opin. Solid State Mater. Sci.*, 2001, **5**, 417–424.
20 A. Čižmek, L. Komunjer, B. Subotić, M. Široki and S. Rončević, *Zeolites*, 1991, **11**, 258.